Dynamics and Hysteresis of the Contact Line between Liquid Hydrogen and Cesium Substrates

E. Rolley and C. Guthmann

Laboratoire de Physique Statistique de l'ENS, associé au CNRS et aux Universités Paris 6 et Paris 7, 24 rue Lhomond, 75005 Paris, France

(Received 16 November 2006; published 20 April 2007)

We have measured both the hysteresis and the dynamics of the edge of a liquid hydrogen meniscus on several solid cesium substrates. We find that the dynamics of the contact line is thermally activated. For all substrates, we find that the activation energy is of the order of the hysteresis. We show that the pinning of the contact line on mesoscopic defects of the Cs substrate is likely to control both the hysteresis and the dynamics of the contact line at low velocity, close to the depinning threshold. Such a mechanism could be relevant also for simple room-temperature systems.

DOI: 10.1103/PhysRevLett.98.166105 PACS numbers: 68.08.Bc, 68.35.Ja

On most solid substrates, the contact angle θ of a sessile drop displays some hysteresis: the drop cannot advance if θ is smaller than a critical value θ_a and cannot recede if $\theta < \theta_r$ [1]. Such a hysteresis is attributed to the heterogeneity of the substrates: the edge of the drop is pinned by the defects, which can be due to chemical heterogeneities or substrate roughness [2]. If a finite velocity $V > 0$ is imposed on the contact line (the contact line advances), then the dynamic contact angle θ_d at macroscopic scale is larger than θ_a and depends on V (if $V < 0$, then $\theta_d < \theta_r$). The dynamics of the contact line (CL) has been investigated for many different systems [3]. At low velocity, when viscous dissipation can be neglected, it has been argued that experimental data are usually consistent with a model of activated dynamics [3]. This has been demonstrated directly in the case of superfluid helium, where the viscosity is negligible and where the temperature can be varied in a large range [4]. In this activated regime, the CL dynamics is controlled by two parameters: the size λ of elementary activated jumps and the activation energy E^* of these jumps.

In the original "molecular-kinetic model," the jumps occur at a molecular scale [5]. λ is microscopic, and E^* is an "activation free energy of wetting"; E^*/λ^2 is expected to be of the order of the energy of adhesion between solid and liquid. The wetting dynamics is controlled by the interactions between the liquid and the substrate and has nothing to do with the hysteresis.

However, for an ordinary (hence disordered) substrate, one can also interpret these jumps as depinning events from the defects of the substrate. Such an interpretation has been used to describe, for instance, the activated motion of magnetic domain walls (see [6], and references therein). In this picture, λ is now the correlation length of the disorder and E^* the typical energy barrier between two pinned configurations of the contact line. The interesting point in this second interpretation is that a *single* physical mechanism controls *both* the hysteresis (or the pinning) of the contact line and its dynamics at the depinning threshold: the activated regime is nothing but a thermal rounding of the depinning transition, as sketched in Fig. 1. Hence, one expects that the hysteresis H scales like E^*:

$$H \equiv \gamma(\cos\theta_r - \cos\theta_a) \sim E^*/\lambda^2, \tag{1}$$

where γ is the liquid-vapor surface tension.

The analog of relation (1) in the context of magnetic domain walls is satisfied for systems with moderate disorder. In these systems, the critical magnetic field (analog of H) is close to the "propagation field" (analog of E^*/λ^2) characterizing the activated regime [7]. To our knowledge, no attempts have been made to check relation (1) or even to correlate hysteresis and dynamics in the context of wetting. In this Letter, we report an experiment designed to investigate the relationship between the hysteresis and the dynamics of the contact line.

System and setup.—We use liquid hydrogen, which does not wet cesium at low temperatures [8,9]. This simple system has a number of advantages for wetting experiments. It is free from chemical contamination: once the substrate is prepared and H_2 is condensed, the cell is closed and the same system can be studied for weeks. The defects

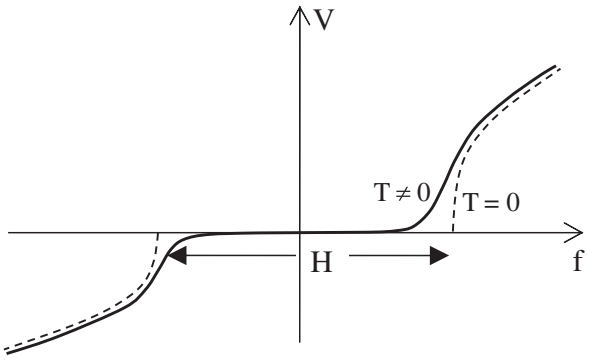

FIG. 1. Velocity-force characteristic: the sharp depinning transition at $T = 0$ (dashed line) is blurred at a finite temperature (solid line). In the case of a contact line, the force f is the unbalanced Young force: $f = \gamma(\cos\theta_{eq} - \cos\theta_d)$, where θ_{eq} is the contact angle at equilibrium.

of the Cs substrates are topographic defects, as the Cs surfaces are prepared at low temperatures by *in situ* evaporation. The roughness of the surface can be modified by varying the evaporation conditions (evaporation rate, substrate temperature, Cs thickness). Previous studies of the dynamics of a superfluid helium meniscus have shown that the length scale of the roughness is of the order of 10 nm [4]. This has been confirmed by direct STM imaging of Cs surfaces [10]. Besides the substrate roughness, the contact angle is an additional parameter which can be tuned between 45° and 0° by increasing the temperature from 14 (H_2 triple point) up to 20 K (wetting temperature for H_2 on Cs). The relevant physical parameters are the surface tension γ and viscosity η ($\gamma = 2.8$ mJ/m^2 and $\eta = 21$ μPa s at 15 K). They are much smaller than those of ordinary liquids, but the ratios γ/η or γ/k_BT have the same order of magnitude than those of water.

The experimental cell is placed in an optical ^{4}He cryostat. After cooling the cell down to 15 K, we start the cesium evaporation. The cesium is deposited on a Si wafer (20×20 mm^2). Two large getters (25 mm long) are used in order to obtain an homogeneous cesium film. For each getter, the mean incidence angle is 20°. The Cs thickness is monitored with a quartz microbalance.

After Cs evaporation, H_2 is condensed into the cell until the liquid level reaches the middle of the nearly vertical cesiated wafer. The wafer is clamped on a translation stage made of a mobile copper plate fixed to two cantilever springs. To the plate is attached a permanent magnet positioned inside a coil. The plate can be displaced by ± 5 mm with a dissipation of a few milliwatts. Such a design allows a perfectly smooth operation. In the present experiment, the plate velocity ranges from 0.3 μm/s up to 3 mm/s. The lower limit is set by the stability of the H_2 liquid level. Real time imaging of the liquid meniscus can be performed during the displacement of the plate. The velocity V of the CL with respect to the plate is obtained by monitoring the position of both the plate and the CL.

In our parameter range, the capillary number Ca, which measures the ratio between viscous forces and capillary forces, is small: $\mathrm{Ca} \equiv \eta V/\gamma < 10^{-5}$. This means that the profile of the meniscus is the same as at equilibrium except in the close vicinity of the contact line. Thus, the dynamic contact angle θ_d can be obtained from the measurement of the capillary rise h of the CL on the plate with respect to the bulk liquid level. The force f per unit length acting on the CL is the unbalanced Young force: $f = \gamma(\cos\theta_{\mathrm{eq}} - \cos\theta_d)$. There is no way to measure θ_{eq}, and f is determined only within a constant.

The bulk liquid level is difficult to determine. Moreover, we have observed long term variation of this level due to slow thermal equilibration of the filling line of the cell. This results in an uncertainty in h of the order of 20 μm, which is the main source of uncertainty for θ_d. However, *variations* of h can be measured very accurately. To do so, we first measure the capillary rise when moving the plate at a constant reference velocity $V_0 = 3$ μm/s and measure the absolute value h_0. Then we repeat the run with the velocity being changed alternatively between V_0 and another value. These jumps in V yield jumps Δh of h which can be measured with an uncertainty of 0.5 μm (Fig. 2). Finally, for $\theta_d \simeq 30°$, the absolute uncertainty on $\cos\theta_d(V_0)$ is $\pm 10^{-2}$, and the relative uncertainty on $\cos\theta_d(V_0) - \cos\theta_d(V)$ is $\pm 5 \times 10^{-4}$.

Three different substrates were used, whose properties are summarized in Table I. For all of them, the evaporation rate is of the order of 3 atomic layers per minute, and the substrate temperature during evaporation is about 80 K (the cell itself remains at 15 K). Annealing over 200 K decreases significantly the hysteresis. For all substrates, the wetting temperature is close to 20 K.

Results and discussion.—A typical curve V vs $\cos\theta_d$ is shown in Fig. 3. The velocity is never actually zero, but the advancing and receding branches are very steep so that the hysteresis can be easily defined. In the following, the hysteresis H will be calculated from the values of θ_d for $V = \pm V_0$.

A log plot of the advancing branch is shown in the inset in Fig. 3: V varies exponentially with $\cos\theta_d$ for more than 3 decades. Such an exponential behavior was observed for all substrates at all temperatures. This shows that the dynamics is activated and that viscous dissipation is not relevant. Indeed, the contribution of viscous dissipation to the change in θ is given by $\theta_d^3 - \theta_{\mathrm{eq}}^3 = 9\,\mathrm{Ca}\,l$, where l is a logarithmic factor [11]. For the highest Ca and the smaller angle, one finds that the change of $\cos\theta_d$ due to viscous dissipation is at most a few 10^{-3} (for the data in Fig. 3, the magnitude of the viscous contribution for $V = 1$ mm/s is of the order of the uncertainty). The dynamics is thus controlled by the rate of depinning events. This process

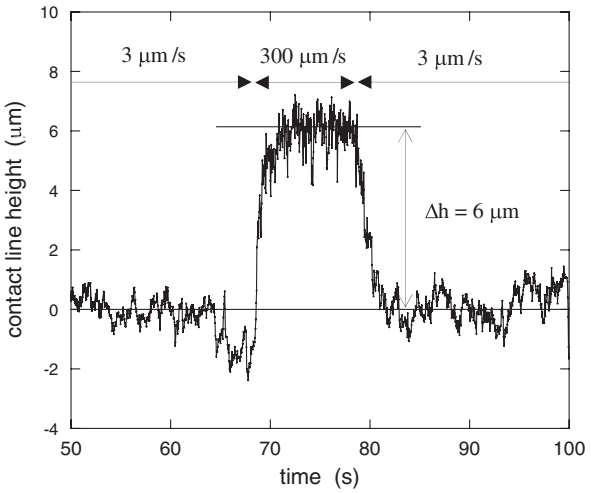

FIG. 2. Height of the meniscus at a function of time t. The plate is drawn out of the liquid bath at the reference velocity $-V_0$ except for $68 < t < 78$ s. In this time interval, the capillary rise is larger by $\Delta h = 6$ μm, which corresponds to a decrease of θ_d by 0.2° [substrate S1 at 15 K: $\theta_d(-V_0) = 29° \pm 2°$].

TABLE I. Properties of cesium substrates. Wetting properties are measured at 15 K.

	Thickness (layers)	Annealing	$\theta_d(3\ \mu\mathrm{m/s})$ (degrees)	H/γ	λ_a (nm)	λ_r (nm)
S1	90	⋯	43 ± 2	0.14	13	10
S2	90	At 250 K	41 ± 2	0.06	19	14
S3	75	At 200 K	46 ± 2	0.16	14	12

is observed only in a narrow range of force close to the depinning threshold, which means that the activation energy or energy barrier E^* is large compared to k_BT. Close to the depinning threshold, one expects V to obey a simple Arrhenius law [5]:

$$|V| = \lambda\nu_0 e^{-E^*/(k_BT)} \exp[\lambda^2|f|/(2k_BT)], \quad (2)$$

where ν_0 is a thermal frequency ($\nu_0 \approx k_BT/h$).

The slope of $\ln|V|$ vs $\cos\theta_d$ yields the activation area λ^2. For all substrates at all temperatures, we have found that λ is significantly larger for an advancing than for a receding CL. So, for each run, $\ln|V|$ is fitted by a linear function $\ln|V| = A + B\cos\theta_d$, and we have allowed the parameters A and B to be different for the advancing and receding cases:

$$B_{a/r} = (\mp)\lambda_{a/r}^2\gamma/(2k_BT), \quad (3)$$

$$A_a = \ln(\lambda_a\nu_0) - [E_a^* - \lambda_a^2\gamma\cos\theta_{\mathrm{eq}}/2]/(k_BT), \quad (4)$$

$$A_r = \ln(\lambda_r\nu_0) - [E_r^* + \lambda_r^2\gamma\cos\theta_{\mathrm{eq}}/2]/(k_BT). \quad (5)$$

Advancing and receding activation lengths λ_a and λ_r are obtained directly from the fitting parameters B_a and B_r. The activation length is found to range from 10 to 20 nm, in agreement with a previous experiment [4] using superfluid helium instead of H_2.

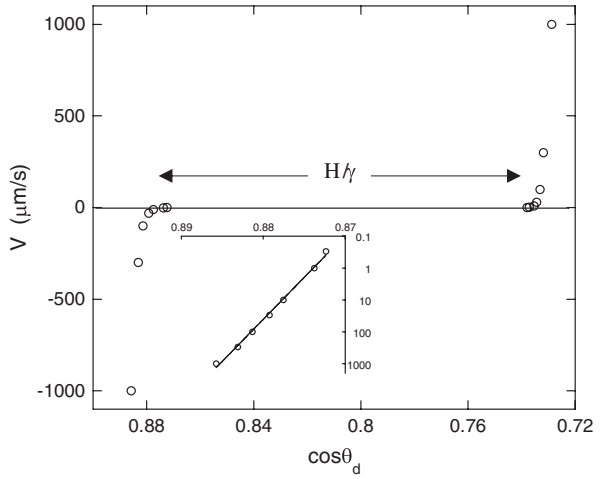

FIG. 3. Velocity V of the contact line as a function of $\cos\theta_d$ (substrate S2 at 15 K). Inset: Semilog plot of the receding branch.

Since θ_{eq} is unknown, the activation energies E_a^* and E_r^* cannot be determined separately from A_a and A_r. The accessible parameter characterizing the mean activation energy is the quantity $\epsilon^* \equiv E_a^*/\lambda_a^2 + E_r^*/\lambda_r^2$. Note that ϵ^* has the dimension of an energy per unit area.

Our main result is summarized in Fig. 4, where ϵ^* is plotted as a function of H. For S2 and S3, ϵ^* has been measured for three different temperatures: ϵ^* is found to increase with T. For all substrates and temperatures, we find that the mean activation energy ϵ^* is of the order of H. This strongly supports the idea that both the wetting hysteresis and the dynamics at a low capillary number are controlled by a single mechanism. The next step is to check whether the values of the activation lengths and energies are consistent with topographic defects of cesium films evaporated at low temperatures.

Direct STM imaging of Cs films prepared approximately in the same conditions as ours has been performed recently [10]. The substrate topography consists in rounded hillocks separated by cusplike valleys. The lateral size of the hillocks is of the order of a few tens of nanometers. This is consistent with the value of the activation length: the hillocks presumably act as pinning defects for the CL. We find also that λ increases when the substrate is annealed above 200 K, which is easily understood: upon annealing, the smallest defects are smeared out by thermal diffusion of Cs atoms.

Relating the substrate topography to the activation energy ϵ^* or the hysteresis H is a more difficult task. For a single topographic defect of size d on a flat surface, one expects that the energy E_s dissipated when the CL moves over the defect is of the order of $\gamma d^2\sin^2\phi[\sin^2\theta_0/(1-\cos\theta_0)]$, where θ_0 is the contact angle on a flat surface and ϕ the maximum local slope of the actual surface with respect to the mean substrate plane [12,13]. This has

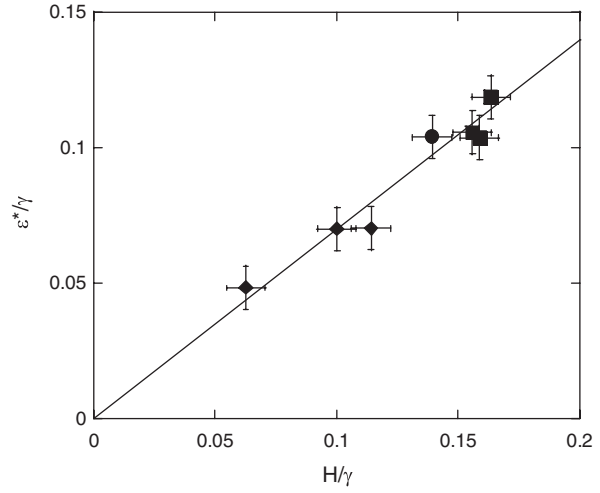

FIG. 4. Normalized mean activation energy ϵ^*/γ as a function of the normalized hysteresis H/γ (substrates S1: ●; S2: ◆; S3: ■). Various points with the same symbols are taken at different temperatures.

TABLE II. Activated dynamics parameters for various liquids on an amorphous fluoropolymer (from Ref. [17]).

Liquid	λ (nm)	$E^*/(\lambda^2\gamma)$	H/γ	W_a/γ
CCl_4	8.1	0.078	0.068	1.53
$(CH_3)_3COH$	9.3	0.078	0.065	1.63
OMCTS	7.0	0.11	0.052	1.77

been checked experimentally for a system of diluted defects for which $H = nE_s$, where n is the density of defects [13]. In order to obtain an estimate for H, we will make the crude assumption that $H \sim nE_s$ still holds for our system where the defects are not diluted. For dense defects ($n \simeq 1/d^2$) and $\theta_0 < 45°$, one finds $H/\gamma \sim (\sin^2\phi)/2$. For our substrates, this leads to a maximum local slope $\phi \sim 15°$; this is quite consistent with the images from Zech *et al.* [10]. Let us also note that, though ϕ is not very large, due to the mesoscopic value of λ, the pinning energy $\lambda^2\epsilon^*$ is of the order of 5×10^5 K. This is much larger than k_BT, as expected from the shape of the V vs $\cos\theta_d$ plot.

Finally, the numerical values of ϵ^* and λ are consistent with the hypothesis that the CL is pinned by topographic defects of the substrate. However, the previous qualitative interpretation does not explain why λ is different for an advancing and a receding CL. Actually, $\theta_a - \theta_r$ varies between 5° and 20°: this is not small compared to ϕ, which means that the shape of the meniscus in the vicinity of the surface is different in an advancing or receding case. The elementary jumps can thus have a different size in both cases. A more precise analysis of the values of ϵ^* and λ requires a better understanding of the CL behavior on a complex topography, as well as taking into account the size distribution of the defects.

Other systems.—Many ordinary systems have been analyzed in the framework of the so-called molecular-kinetic model [3,14]. In this approach, Eq. (2) still holds, but E^* characterizes the energy barriers involved in molecular adsorption or desorption process, and it has been argued by Blake and De Coninck that $E^* \simeq \lambda^2 W_a$, where $W_a \equiv \gamma(1 + \cos\theta_{eq})$ is the work of adhesion [15].

Such an interpretation can make sense if λ, which is now a mean distance between adsorption sites, is microscopic. Indeed, λ is found to be of the order of or smaller than 1 nm, for instance, for such systems as polar liquid (water, water + glycerol) on polymers such as polyethylene terephtalate [16] (see Refs. [3,14] for more extensive references). However, Petrov *et al.* found λ close to 8 nm for simple liquids on amorphous fluoropolymers [17]. In this later case, a true molecular mechanism is not very likely. Moreover, the work of adhesion W_a is found to be much larger than E^*/λ^2, which enters in an *exponential* factor in Eq. (2). For these systems, it is more likely that the disorder of the amorphous layer controls the value of activation energy, in analogy with the H_2-Cs system. As shown in Table II, one finds indeed that the hysteresis is of the order of E^*/λ^2.

In conclusion, using nonconventional systems, we have shown that the pinning of the contact line on mesoscopic defects is likely to control both the wetting hysteresis and the activated dynamics which is observed close to the depinning threshold. This interpretation is consistent with experimental data on simple systems at room temperature, when the activation length is mesoscopic. When the activation length is found to be microscopic, the underlying description of the contact line as a continuous elastic system breaks down. However, if the system if simple enough to be controlled by a single adsorption or desorption mechanism (no slow diffusion in the liquid or the substrate, no large defects, etc.), then the hysteresis should still be of kinetic origin, as proposed by Blake himself [14]. At present, this hypothesis is difficult to test: published work on the CL dynamics does not report on, or even consider, the hysteresis. Moreover, calculated values of activation energies often rely on *ad hoc* assumptions for the value of the equilibrium contact angle. We hope that our work will trigger further examination of available data.

We are very grateful to the low-temperature group of Konstanz University for many discussions and for providing us results prior to publication. We acknowledge the help of Olivier Gareil in the experiment and fruitful discussions with Jacques Ferré.

[1] R. H. Detree, in *Wettability*, edited by J. C. Berg (Dekker, New York, 1993).
[2] P. G. De Gennes, Rev. Mod. Phys. **57**, 827 (1985).
[3] T. D. Blake, J. Colloid Interface Sci. **299**, 1 (2006).
[4] A. Prevost, C. Guthmann, and E. Rolley, Phys. Rev. Lett. **83**, 348 (1999).
[5] T. D. Blake and J. M. Haynes, J. Colloid Interface Sci. **30**, 421 (1969).
[6] J. Ferré, in *Spin Dynamics in Confined Magnetic Structures I*, edited by B. Hillebrands and K. Ounadjela, Topics Appl. Phys. Vol. 83 (Springer-Verlag, Berlin, 2002), p. 127.
[7] A. Kirilyuk *et al.*, J. Magn. Magn. Mater. **171**, 45 (1997).
[8] D. Ross, P. Taborek, and J. E. Rutledge, Phys. Rev. B **58**, R4274 (1998).
[9] M. Pettersen *et al.*, J. Low Temp. Phys. **134**, 281 (2004).
[10] M. Zech *et al.*, J. Low Temp. Phys. **137**, 179 (2004).
[11] R. G. Cox, J. Fluid Mech. **168**, 169 (1986).
[12] J. F. Joanny and P. G. De Gennes, J. Chem. Phys. **81**, 552 (1984).
[13] S. Ramos *et al.*, Phys. Rev. E **67**, 031604 (2003).
[14] T. D. Blake, in Wettability (Ref. [1]).
[15] T. D. Blake and J. De Coninck, Adv. Colloid Interface Sci. **96**, 21 (2002).
[16] R. A. Hayes and J. Ralston, J. Colloid Interface Sci. **159**, 429 (1993).
[17] J. G. Petrov *et al.*, Langmuir **19**, 2795 (2003).